Journal of Organometallic Chemistry, 429 (1992) 379–389
Elsevier Sequoia S.A., Lausanne
JOM 22469

Synthesis, characterization, crystal structure, and solution conformation of $(-)_{436}$-(S_{Co},S_C)-$(\eta^5$-$C_9H_7)Co^*(C_3F_7)I(Ph_2PNHC^*H(CH_3)Ph)$, an easily resolvable chiral-at-metal complex

Chet Jablonski, Zhongxin Zhou and John N. Bridson
Department of Chemistry, Memorial University, St. John's, Newfoundland A1B 3X7 (Canada)

(Received August 21, 1991)

Abstract

A convenient method for the preparation and resolution of $(-)_{436}$-(S_{Co},S_C)-$(\eta^5$-$C_9H_7)Co^*(C_3F_7)I(Ph_2PNHC^*H(CH)_3Ph)$ (**2a**) from racemic $(\eta^5$-$C_9H_7)CO^*(C_3F_7)(CO)I$ with an optical yield >99% is described. The absolute configuration of **2a** was determined by crystallography. $(-)_{436}$-**2a** crystallizes in the space group $P2_12_12_1$ with $a = 16.362(1)$, $b = 19.944(4)$, $c = 9.417(2)$ Å, $V = 3073.0(8)$ Å^3, $Z = 4$, $R = 0.071$, $R_w = 0.064$.

Introduction

Chiral-at-metal, pseudo-octahedral, three legged "piano stool" complexes are excellent templates for stoichiometric asymmetric synthesis and have therefore been extensively studied [1]. Previous work in this laboratory [2] has demonstrated that diastereoselective Arbuzov dealkylation of prochiral phosphonite complexes η^5-$CpCo^*I(P^*$-donor$)(PR(OR')_2)^+$ formed *in situ* by iodide substitution of $CpCo^*I_2(P^*$-donor$)$ proceeds with good to excellent optical yields. Our studies of $M^* \rightarrow P_\alpha$ chiral induction were, however, complicated by the formation of epimeric Co^* centres in the substitution step which led ultimately to a mixture of four diastereomeric products. We therefore sought to prepare a mono-halogenated, Co-chiral substrate which would allow a simplified stereochemical assay. Here we report the facile synthesis of the chiral, perfluoro alkyl η^5-indenyl analog **2a** which is easily resolved in gram quantities by a second order asymmetric transformation [3].

Results and discussion

A Co-epimeric mixture of the title complex **2a, b** was synthesized in high yield by substitution of carbon monoxide in racemic **1** by the chiral aminophosphine

Correspondence to: Dr. C. Jablonski, Department of Chemistry, Memorial University, St. John's, Newfoundland A1B 3X7, Canada.

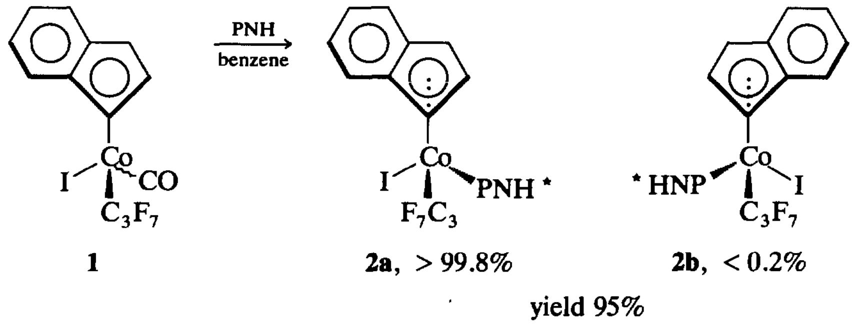

Scheme 1.

(*S*)-(−)diphenyl((1-phenylethyl)amino)phosphine (PNH*) [4] at room temperature in benzene solution (Scheme 1). Sublimation of benzene solvent at 0°C/0.1 Torr affords the crude product as a dark red-brown powder in 95% yield. TLC and ^{1}H NMR analysis show that the crude product is in fact a single diastereomer (> 99.8% **2a** and < 0.2% **2b** by integration of ^{1}H NMR doublets of C*–Me at 1.25 and 0.90 ppm). In this synthesis the optical yield is therefore equal to the chemical yield.

That resolution occurs during workup was established by three independent experiments: (i) NMR reactions at ambient temperature in benzene-d_6 establish that the reaction of **1** with PNH* is very rapid, and complete conversion to **2** occurs during mixing to afford **2b**:**2a** in a kinetic product ratio of 46:54 at 22°C; (ii) variable temperature equilibrium concentration measurements of **2b**:**2a** by ^{1}H NMR in benzene-d_6 give $\Delta H = 2.6 \pm 0.2$ kJ mol^{-1} and $\Delta S = 7.2 \pm 0.7$ J K^{-1} mol^{-1} for K_{eq} = **2b**/**2a** giving a calculated equilibrium ratio for **2b**/**2a** of 44:56 at +5°C; and (iii) workup of the reaction by sublimation of benzene solvent at low temperature (−11°C) to avoid formation of liquid phase afforded a 34:66 Co-epimeric mixture of **2b**:**2a**. Isolation of a single diastereomer by sublimation at 0°C (Experimental section) is therefore the result of a second-order asymmetric transformation [3] which occurs during workup. Freezing point depression from the dissolved epimeric mixture **2a**, **b** provides for the presence of a small volume of liquid phase benzene at 0°C in which fractional crystallization of the less soluble diastereomer **2a** occurs, replenished by shifting the Co epimerization equilibrium **2b** ⇌ **2a**.

The structure of **2a**, **b** was established spectroscopically, and in the case of **2a** via a single crystal X-ray study. ^{1}H NMR resonances for the indenyl H_1 (see Fig. 5 below for indenyl ring numbering) and for CH_3 on PNH* are clearly distinguishable for the two diastereomers **2a** and **2b** (**2a**: δ 4.50 (H_1), 1.25 ppm (d, CH_3, $^3J = 6.54$ Hz); **2b** δ 4.64 (H_1), 0.90 ppm (d, CH_3, $^3J = 6.54$ Hz)), see Experimental section. The ring carbons $C_{1,3}$, $C_{5,6}$, $C_{4,7}$ and $C_{3a,7a}$ as well as $C_\alpha F_2$ and $C_\beta F_2$ fluorine atoms are rendered diastereotopic by the chiral Co^{III} center, and distinct ^{13}C and ^{19}F resonances are observed for all.

Figure 1 shows the solid state structure of complex **2a**, determined by X-ray diffraction methods on a single crystal of **2a** grown by slow diffusion of hexane onto a CH_2Cl_2 solution. Attempts made to model a disorder involving two

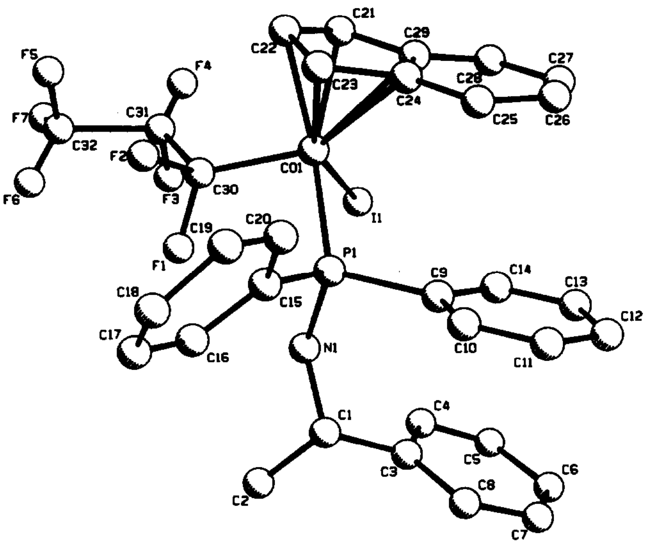

Fig. 1. Molecular structure of **2a**.

conformations of the C_3F_7 group which became apparent on refinement were unsuccessful. Although giving a reduced R value, thermal parameters calculated throughout the molecule were unreasonable. Therefore the structure was refined assuming the presence of a single, major conformation for the C_3F_7 group. This approach resulted in large B_{eq} values for several atoms in C_3F_7 and a final Fourier difference map which showed significant peaks in the area of C_3F_7. Selected bond angles and bond distances are given in Table 1. Atomic coordinates are given in

Table 1

Selected bond distances (Å) and bond angles (deg) for **2a**

Distances				Angles	
I–Co	2.599(2)	C21–C22	1.39(3)	I–Co–P	95.7(1)
Co–P	2.275(5)	C21–C29	1.41(3)	I–Co–C21	92.3(6)
Co–C21	2.11(2)	C22–C23	1.36(2)	I–Co–C22	128.3(8)
Co–C22	2.07(2)	C23–C24	1.42(2)	I–Co–C23	153.8(5)
Co–C23	2.06(1)	C24–C25	1.45(2)	I–Co–C24	120.7(5)
Co–C24	2.30(2)	C24–C29	1.44(2)	I–Co–C29	90.7(5)
Co–C29	2.26(2)	C25–C26	1.38(2)	I–Co–C30	94.61(8)
Co–C30	1.962(2)	C26–C27	1.41(3)	P–Co–C21	157.2(6)
P–N	1.68(1)	C27–C28	1.38(3)	P–Co–C22	135.8(8)
N–C1	1.46(2)	C28–C29	1.35(3)	P–Co–C23	99.8(6)
				P–Co–C24	94.5(4)
				P–Co–C29	121.1(6)
				P–Co–C30	90.9(1)
				C21–Co–C30	109.8(7)
				C22–Co–C30	90.3(6)
				C23–Co–C30	106.1(6)
				C24–Co–C30	143.4(5)
				C29–Co–C30	146.9(6)

Table 2

Atomic coordinates and B_{eq} for **2a**

$$B_{eq} = 8\frac{\pi^2}{3}\sum_{i=1}^{3}\sum_{j=1}^{3} U_{ij} a_i^* a_j^* \vec{a}_i \vec{a}_j$$

Atom	x	y	z	B_{eq}
I(1)	0.24379(7)	0.20943(7)	0.1436(1)	5.37(6)
Co(1)	0.1131(1)	0.2751(1)	0.0713(2)	3.6(1)
P(1)	0.1242(2)	0.2544(2)	−0.1655(5)	3.2(2)
F(1)	0.2252(7)	0.3660(6)	−0.054(1)	9.9(4)
F(2)	0.1120(7)	0.4151(5)	−0.009(1)	8.6(3)
F(3)	0.272(1)	0.375(1)	0.158(2)	22.9(8)
F(4)	0.1855(8)	0.3808(6)	0.263(1)	9.6(4)
F(5)	0.151(1)	0.497(1)	0.183(2)	21.1(8)
F(6)	0.242(1)	0.4951(8)	0.051(2)	13.6(5)
F(7)	0.275(1)	0.489(1)	0.246(3)	22.4(8)
N(1)	0.2213(6)	0.2540(6)	−0.223(1)	3.1(6)
C(1)	0.2494(9)	0.2279(7)	−0.359(2)	3.6(7)
C(2)	0.3201(9)	0.2689(9)	−0.413(2)	6(1)
C(3)	0.2722(8)	0.1526(8)	−0.354(2)	3.8(8)
C(4)	0.318(1)	0.130(1)	−0.236(2)	5(1)
C(5)	0.340(1)	0.062(1)	−0.231(2)	5(1)
C(6)	0.311(1)	0.017(1)	−0.335(3)	6(1)
C(7)	0.264(2)	0.040(1)	−0.446(3)	9(2)
C(8)	0.243(1)	0.109(1)	−0.461(2)	5(1)
C(9)	0.0825(8)	0.1735(8)	−0.228(2)	2.9(8)
C(10)	0.031(1)	0.1647(9)	−0.334(2)	4(1)
C(11)	0.004(1)	0.105(1)	−0.376(2)	5(1)
C(12)	0.034(1)	0.048(1)	−0.301(2)	6(1)
C(13)	0.087(1)	0.057(1)	−0.190(2)	5(1)
C(14)	0.116(1)	0.1164(9)	−0.148(2)	4.4(9)
C(15)	0.0699(9)	0.3153(7)	−0.280(2)	3.0(8)
C(16)	0.1131(8)	0.3623(8)	−0.364(2)	4.1(9)
C(17)	0.075(1)	0.4097(8)	−0.447(2)	5(1)
C(18)	−0.008(1)	0.4089(9)	−0.455(2)	5(1)
C(19)	−0.053(1)	0.366(1)	−0.366(2)	6(1)
C(20)	−0.017(1)	0.320(1)	−0.286(2)	5(1)
C(21)	0.064(1)	0.268(1)	0.278(2)	6(1)
C(22)	0.028(1)	0.320(1)	0.202(3)	7(2)
C(23)	−0.010(1)	0.297(1)	0.083(2)	5(1)
C(24)	−0.0142(8)	0.227(1)	0.092(2)	4(1)
C(25)	−0.058(1)	0.178(1)	0.006(2)	5(1)
C(26)	−0.053(1)	0.113(1)	0.057(2)	6(1)
C(27)	0.000(1)	0.094(1)	0.168(3)	7(1)
C(28)	0.040(1)	0.143(2)	0.244(2)	9(2)
C(29)	0.036(1)	0.209(1)	0.213(2)	5(1)
C(30)	0.1697	0.3612	0.0489	7.8(6)
C(31)	0.2072	0.3936	0.1792	–
C(32)	0.2119	0.4788	0.1440	39(5)
H(1)	0.2615	0.2724	−0.1617	3.7
H(2)	0.2058	0.2325	−0.4250	4.3
H(3)	0.3636	0.2669	−0.3468	6.8
H(4)	0.3376	0.2517	−0.5019	6.8
H(5)	0.3030	0.3142	−0.4244	6.8
H(6)	0.3331	0.1604	−0.1627	5.8
H(7)	0.3756	0.0469	−0.1570	6.0

Table 2 (continued)

Atom	x	y	z	B_{eq}
H(8)	0.3234	−0.0295	−0.3273	7.2
H(9)	0.2454	0.0094	−0.5148	10.9
H(10)	0.2115	0.1246	−0.5380	5.8
H(11)	0.0122	0.2033	−0.3840	4.9
H(12)	−0.0344	0.1014	−0.4512	6.6
H(13)	0.0178	0.0040	−0.3292	7.2
H(14)	0.1047	0.0188	−0.1399	5.6
H(15)	0.1540	0.1212	−0.0741	5.2
H(16)	0.1710	0.3608	−0.3633	4.9
H(17)	0.1055	0.4425	−0.4971	6.4
H(18)	−0.0357	0.4372	−0.5198	5.5
H(19)	−0.1110	0.3698	−0.3624	6.6
H(20)	−0.0491	0.2892	−0.2314	6.3
H(21)	0.0988	0.2711	0.3568	7.6
H(22)	0.0291	0.3657	0.2297	7.7
H(23)	−0.0299	0.3239	0.0060	5.5
H(24)	−0.0880	0.1895	−0.0769	6.5
H(25)	−0.0861	0.0801	0.0137	7.0
H(26)	0.0077	0.0476	0.1899	8.5
H(27)	0.0726	0.1290	0.3223	9.9

Table 2. The coordination geometry is best described as a distorted octahedron with η^5-indenyl occupying three *facial* coordination sites. I–Co–P, I–Co–C(30), and P–Co–C(30) interligand bond angles approximate to 90°. The 5-membered ring of the η^5-indenyl ligand in **2a** shows small but characteristic distortions from planarity in the solid state [5]. A Co displacement towards C_1–C_3 (Δ_{M-C} defined as $d(\text{Co–C}_{3a}, \text{C}_{7a})–d(\text{Co–C}_1, \text{C}_3)$ is 0.2 Å) as well as a hinge angle of 10.79° between the planes defined by C_1–C_2–C_3 and C_1–C_3–C_{3a}–C_{7a} and a fold angle of 14.93° between the plane C_1–C_2–C_3 and the best plane containing C_{3a}–C_4–C_5–C_6–C_7–C_{7a} are consistent with a pronounced "slip fold" distortion. Comparison of the ^{13}C chemical shift difference ($\Delta\delta(^{13}\text{C}) = \delta\text{C}_{\text{C3a,C7a}(\eta\text{-indenyl})} - \delta\text{C}_{\text{C3a,7a(indenyl sodium)}}$) of **2a** with the results of Baker and Marder [5] suggests that this distortion persists in solution. The calculated chemical shift difference parameters, $\Delta\delta\text{C}_{\text{C3a}} = -18.17$ and $\Delta\delta\text{C}_{\text{C7a}} = -18.99$, for **2a** show that the indenyl ligand in **2a** is located in the distorted η^5 range.

Figures 1 and 2 show that **2a** adopts a solid state conformation in which two ligand phenyl rings "stacks" with the indenyl aromatic ring. The mean distance between the best plane defined by the phenyl rings C9–C14 and C24–C29 is 3.28(2) Å with a dihedral angle of (3.0°) defined by a slight tilt of C24–26 toward the plane of C9–C14. The mean interplanar distances from C3–C8 to the best plane of C9–C14 is 3.43(2) Å with dihedral angle of 15.4°. The measured interplanar distances are comparable to those of graphite (3.35 Å).

Reference to the crystal structure of Fig. 1 shows that the absolute configuration of $(-)_{436}$-**2a** is S_{Co} based on the modified CIP [6] preference I > η^5-indenyl > PNH* > R_f. The CD spectrum of **2a** is shown in Fig. 3; however, owing to stereochemical lability at Co, we were unable to isolate diastereomerically pure **2b** for comparison.

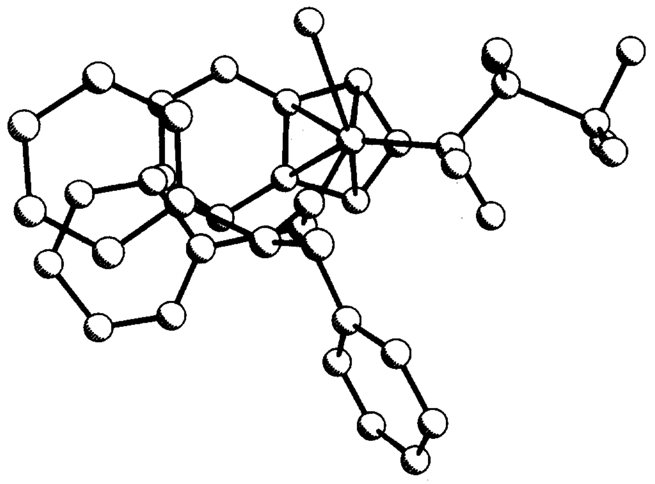

Fig. 2. Molecular structure of **2a** (top view).

Chemical shift assignments and solution conformation of **2a** were investigated using ^{1}H nuclear Overhauser effect difference spectra (NOED) at -30°C in order to minimize Co-epimerization [7]. Figure 4 shows ^{1}H NOED spectra of **2a** obtained at 300 MHz on a sample containing *ca.* 20% isomer **2b**. Spectra b, d, and e allow assignments of the η^5 ring protons, H_1–H_3 (cf. Experimental). Spectrum d shows strong correlations of the signal assigned to H_2 at 5.65 ppm with the signals at 6.63 and 4.50 ppm which are then confidently assigned to H_3 and H_1. Spectrum b correlates $H_3 \rightarrow H_2$ while spectrum e confirms the assignments of H_1 and H_2. Considerable degeneracy is observed in the aromatic region. However, spectra f and g locate nonisochronous C*H(Me)*Ph ortho* protons in the multiplets at 6.76 ppm (integration 3H, overlapped with H_3 and an unassigned phenyl proton) and 7.87 ppm (integration 2H, overlapped with H_7) implying a restricted C*–Ph phenyl rotation. Restricted rotation of one of the diastereotopic PPh_2 rings which is

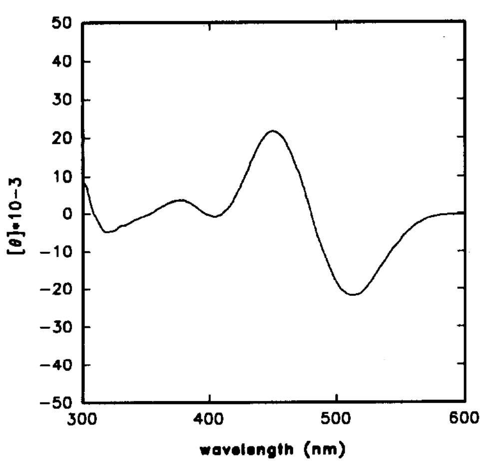

Fig. 3. Circular dichroism (CD) spectrum of **2a**.

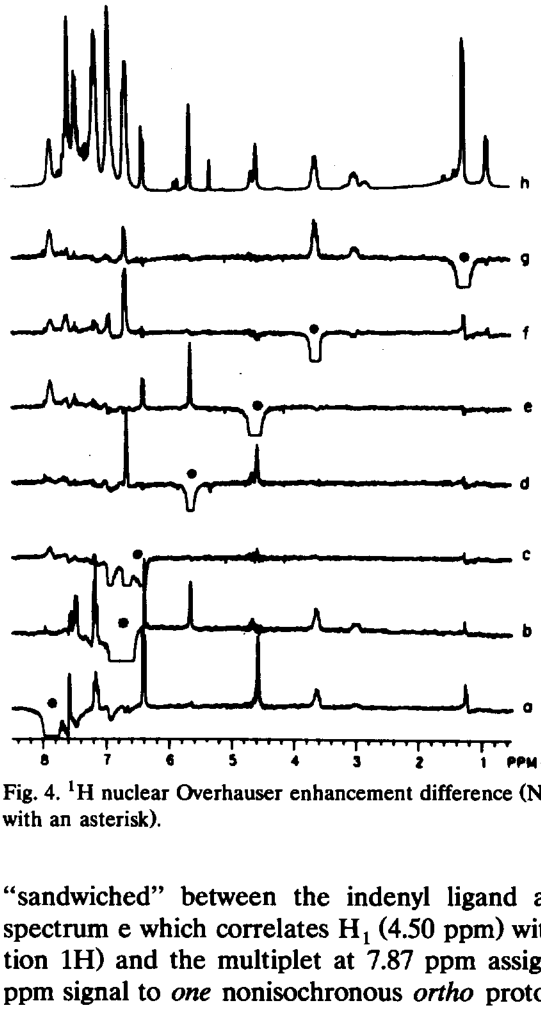

Fig. 4. ^{1}H nuclear Overhauser enhancement difference (NOED) spectra of **2a** (irradiated peak marked with an asterisk).

"sandwiched" between the indenyl ligand and C*–Ph is also apparent from spectrum e which correlates H_1 (4.50 ppm) with the doublet at 6.42 ppm (integration 1H) and the multiplet at 7.87 ppm assigned to H_7. Assignment of the 6.42 ppm signal to *one* nonisochronous *ortho* proton of a diastereotopic PPh_2 group is consistent with restricted phenyl rotation arguments presented above and suggests a solution conformation which places PNH* *syn* to the ring junction (C_{7a}) similar to what is observed in the solid state, *cf*. Fig. 5. Variable temperature NMR experiments on **2a** were carried out to search for phenyl rotation leading to coalescence behaviour of the nonequivalent o-C_6H_5 resonances of P–Ph at 6.42 and C–Ph at 7.87 ppm. These experiments were limited by facile Co epimerization leading to an equilibrium mixture **2a, b** and sample deterioration at the upper temperature limit. Examination of spectra recorded at 25–80°C in C_6D_6 showed no line broadening associated with site exchange. The remaining NMR assignments follow from consideration of splitting patterns (cf. Experimental section).

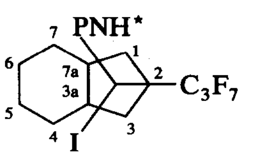

Fig. 5. Solution conformation of **2a**.

The facile preparation of resolved **2a** and the presence of a reactive Co–I bond suggest use as an organometallic chiral synthon. However, such applications of **2a** are severely limited by facile Co epimerization. Preliminary kinetic studies indicate that diastereomerically pure **2a**, like the related CpCo*(L–L*)X containing labile X reported by Brunner [8], epimerizes readily by a dissociative mechanism to give an approximately 50:50 equilibrium mixture of **2b**:**2a**. The approach to equilibrium in benzene solution follows clean first order kinetics at 22–80°C. However the measured first order rate constants measured by NMR are irreproducible with values ranging from 10^{-6} to 10^{-4} s^{-1} at 22°C. A single electron mechanism [9*] involving homolysis of the Co–halide bond may be responsible.

Experimental

General

All manipulations were carried out under prepurified argon or dinitrogen using standard Schlenk techniques. THF and benzene were freshly distilled from deep purple solutions of sodium benzophenone ketyl. (*S*)-(−)diphenyl((1-phenylethyl) amino)phosphine (PNH*) was prepared using literature methods [4] from commercial (Aldrich) (*S*)-(−)diphenyl((1-phenylethyl)amine and diphenylchlorophosphine. n-C_3F_7I (Aldrich) was used as received. Technical grade indene and 1,5-cyclooctadiene (COD) were distilled at 54°C/5 Torr and 57°C/30 Torr, respectively, before use. η^5-$C_9H_7Co(CO)_2$ was prepared using a modification of the literature method [10,11] described below. NMR spectra were measured on a GE 300-NB instrument. Chemical shifts are reported in ppm with respect to internal TMS (^1H), $CFCl_3$ (^{19}F), or $CDCl_3$ solvent (77.0 ppm) in the case of the ^{13}C data. IR spectra were measured as neat films cast on KBr disks or as CH_2Cl_2 solutions in KBr cells on a Mattson Polaris instrument. Proton NOED spectra were determined at −30°C in CD_2Cl_2 under steady state conditions as descirbed previously [2]. Melting points were determined under dinitrogen in sealed capillaries and are uncorrected. Elemental analyses were determined by Guelph Chemical Laboratories, Ontario. Optical rotation measurements were determined in methylene chloride (*ca.* 1 mg/ml) in a 1 cm path length cell with a Perkin–Elmer Model 241 polarimeter. Circular dichroism (CD) spectra were determined in methylene chloride (*ca.* 1 mg/mL) on a Jasco J 40 A apparatus using a 0.1 cm path length cell.

Crystal structure determination

Crystal data were collected at ambient temperature on a Rigaku AFC6S diffractometer with graphite monochromated Mo-K_α radiation (λ = 0.71069) and a 2 KW sealed tube generator, using the ω–2θ scan technique to a maximum 2θ value of 50.0°. Cell constants and an orientation matrix for data collection were obtained from a least-squares refinement using the setting angles of 25 carefully centered reflections in the range $31.26 < 2\theta < 40.68°$. The structure was solved by direct methods using TEXAN software (Molecular Structure Corporation). Data from two octants were collected and redundant reflections removed during solution and preliminary refinement. Final rounds of refinement included hydrogen

* Reference number with asterisk indicates a note in the list of references.

Table 3

Summary of crystallographic data for **2a**

Formula	$C_{32}H_{27}CoF_7INP$
F.W. ($g\ mol^{-1}$)	775.37
Crystal habit	black rectangular plate
Crystal size (mm)	0.37×0.27×0.08
Crystal system	Orthorhombic
No. of reflections used for unit cell determination	25
2θ range (°)	31.3–40.7
Omega scan peak width at half-height	0.27
Lattice parameters	
a (Å)	16.362(1)
b (Å)	19.944(4)
c (Å)	9.417(2)
V (Å^3)	3073.0(8)
Space group	$P2_12_12_1$ (No. 19)
Z	4
D_{calc} ($g\ cm^{-3}$)	1.676
$F(000)$	1536
μ(Mo-K_α) (cm^{-1})	16.66
Scan width (deg)	$0.89+0.30\tan\theta$
$2\theta_{max}$ (deg)	50.0
No. reflections measured	
total	6184
unique	3092
R_{int}	0.055
Corrections	Lorentz polarization (trans. factors: 0.77–1.00)
Function minimized	$\Sigma w(\lvert F_o\rvert - \lvert F_c\rvert)^2$
Least squares weights	$4F_o^2/\sigma^2(F_o^2)$
p factor	0.01
Anomalous dispersion	All non-hydrogen atoms
No. of observations ($I > 3.00\sigma(I)$)	3415
No. of variables	329
Reflection/parameter ratio	10.38
R	0.071
R_w	0.064

atoms at calculated positions with thermal parameters set 20% greater than those of the connected atoms. Absolute configuration was determined by refining both enantiomers to convergence on the complete data set with anomalous dispersion corrections included. The configuration of Fig. 1 refined to a value of 0.6% lower than its enantiomer. Since the correct hand (S) was obtained for the chiral carbon derived from commercial (S)-(−)-diphenyl((1-phenylethyl)amine, we are confident that the assignment of absolute configuration at cobalt is correct. Further details are given in Table 3.

η^5-$C_9H_7Co(CO)_2$. Finely divided lithium (1.50 g, 0.219 mol) was suspended in 250 mL of dry THF under argon. The mixture was heated at 65°C in an oil bath and a mixture of indene (30.5 g, 0.263 mol) and 1,5-cyclooctadiene (27.8 g, 0.258

mol) was slowly added with stirring. Continued stirring for 1 h resulted in a yellow solution. The oil bath was removed and anhydrous $CoCl_2$ (13.9 g, 0.107 mol) added slowly over a 25 minute period. This stage of the reaction is vigorously exothermic. The solution was stirred for an additional 30 min. The resulting dark red-brown solution was cooled to room temperature and filtered through a Schlenk filter fitted with a 5 cm silica gel plug. Removal of volatiles in an oil pump vacuum at 40°C left a dark residue which was taken up in 200 mL of hexane and stirred under an atmosphere of CO at room temperature for 90 min. Filtration through a short plug of silica gel and removal of volatiles in oil pump vacuum (0.1 Torr) gave the crude product as an air-sensitive, deep red-brown oil (22.1 g, 90%). IR: ν(CO), 2020, 1960 cm^{-1}.

η^5-$C_9H_7Co(C_3F_7)I(CO)$ (1). A slight excess (4.30 g, 14.5 mmol) of perfluoropropyl iodide (C_3F_7I) was added via a syringe at room temperature to a solution of 3.30 g (14.3 mmol) of η^5-$C_9H_7Co(CO)_2$ in 100 mL benzene under an atmosphere of N_2. Continued stirring at room temperature for 40 h resulted in the formation of a dark red-brown solution containing some black precipitate. The precipitate was collected on a glass frit, washed with a small amount of hexane and redissolved in CH_2Cl_2. Removal solvent (water aspirator followed by oil pump vacuum) left the crude product as an air-stable black powder. Additional product was recovered by chromatography of the filtrate on a 300 × 35 mm silica gel column (2:1 benzene:hexane elution) to give a total yield of 5.71 g (80%) of **1**, m.p. > 120°C (dec.). Anal. Calc. for $C_{13}H_7OCoF_7I$ (Found); C, 31.35 (31.71), H, 1.42 (1.83)%. IR: ν(CO), 2081 cm^{-1}. ^{1}H NMR ($CDCl_3$): δ 5.80 (s, 1H, H_1), 5.90 (s, 1H, H_2), 6.84 (s, 1H, H_3), 7.74 (d, J = 8.5, 1H, H_4), 7.62 (t, J = 8.50, 1H, H_5), 7.53 (d, J = 8.50, 1H, H_7), 7.43 (t, J = 8.50, 1H, H_6). ^{13}C NMR ($CDCl_3$): δ 71.94 (C_1), 95.37 (C_2), 87.95 (C_3), 111.65, 109.46 (C_{3a}, C_{7a}), 133.12 (C_5), 132.31 (C_6), 128.72 (C_4), 124.32 (C_7), 197.78 (CO). ^{19}F NMR ($CDCl_3$): δ −47.59 (d, ^2J = 208.1, $C_\alpha F_a F_b$), −51.15 (d, ^2J = 208.1, $C_\alpha F_a F_b$), −111.94 (d, ^2J = 277.9, $C_\beta F_a F_b$), −115.70 (d, ^2J = 277.9, $C_\beta F_a F_b$), −79.73 (s, CF_3).

η^5-$C_9H_7Co(C_3F_7)I(PNH^*)$ (2a), method A. A solution of (*S*)-(−)-diphenyl ((phenylethyl)amino)phosphine (PNH*, 0.564 g, 1.85 mmol) in 15 mL benzene was added slowly to a solution of **1** (0.921 g, 1.85 mmol) in 30 mL benzene at room temperature. After stirring for 30 min, the solution was placed in an ice bath for 10 min and the benzene solvent removed by sublimation in an oil pump vacuum to afford a dark red-brown powder (1.37 g, 95%). TLC (elution with THF:hexane 1:5) and ^{1}H NMR analysis indicated the presence of a single isomer, which was shown to be **2a**. The crude product was crystallized at −20°C from CH_2Cl_2/hexane under a dinitrogen atmosphere to give pure **2a** as well formed, rectangular black crystals, m.p. 132°C (dec.). Anal. Calc. for $C_{32}H_{27}CoF_7INP$ (Found); C, 49.57 (49.21), H, 3.51 (3.23), N, 1.81 (1.82)%. ^{1}H NMR ($CDCl_3$): **2a** δ 4.50 (s, 1H, H_1), 5.65 (s, 1H, H_2), 6.63 (m, 2H, H_3 and *o*-C-C_6H_5), 6.42 (d, 1H, *o*-PC_6H_5), 7.87 (m, 2H, H_7 and *o*-C-C_6H_5), 3.66 (m, 1H, C*H), 2.98 (m, 1H, NH), 1.25 (d, J = 6.5, 3H, CH_3); **2b** δ 4.64 (m, 1H, H_1), 5.65 (m, 1H, H_2), 6.40–7.90 (C_6H_5), 3.66 (m, 1H, C*H), 2.82 (m, 1H, NH), 0.90 (d, J = 6.5, 3H, CH_3). ^{13}C NMR ($CDCl_3$): **2a** δ 72.56 (C_1), 94.82 (d, J = 8.1, C_2), 78.57 (d, J = 9.4, C_3), 112.53, 111.71 (C_{3a}, C_{7a}), 124.35–145.63 (C_6H_5), 54.69 (d, J = 12.4, CH), 27.24 (d, J = 3.2, CH_3). ^{19}F NMR ($CDCl_3$): **2a** δ −58.17 (d, ^2J = 247.7, $C_\alpha F_a F_b$,), −58.57 (d, ^2J = 247.7, $C_\alpha F_a F_b$) −107.86 (d, ^2J = 277.3, $C_\beta F_a F_b$), −112.19 (d, ^2J = 277.3, $C_\beta F_a F_b$), −79.96 (s,

CF_3). Polarimetric data, $[\alpha]$ (λ): $-320°$ (579 nm), $-670°$ (546 nm), $-1100°$ (436 nm).

η^5-$C_9H_7Co(C_3F_7)I(PNH^*)$ (2a), method B. A solution of (*S*)-(−)-diphenyl ((phenylethyl)amino)phosphine (PNH*, 0.016 29 g, 0.053 35 mmol) in 3 mL benzene was added slowly to a solution of **1** (0.023 77 g, 0.047 73 mol) in 4 mL benzene at room temperature. After stirring for 10 min, the solution was placed in a refrigerated bath at −11°C. After the solvent was frozen benzene was removed by sublimation in oil pump vacuum over 48 h. 1H NMR analysis showed that the crude product contained a 34:66 mixture of **2b**:**2a**.

Acknowledgments

We thank the Natural Sciences and Engineering Research Council of Canada (NSERC) for a grant in support of this work. Z.Z. acknowledges Memorial University for a graduate fellowship.

References and notes

1 G.J. Baird, J.A. Bandy, S.G. Davies and K. Prout, J. Chem. Soc., Chem. Comm., (1983) 1202; S.G. Davies and J.I. Seeman, Tetrahedron Lett., 25 (1984) 2709; S.G. Davies and J.I. Seeman, Tetrahedron Lett. 25 (1984) 1845; G.J. Baird, S.G. Davies, R.H. Jones, K. Prout and P.J. Warner, J. Chem. Soc., Chem. Comm., (1984) 751; S.G. Davies, I.M. Dordor and P.J. Warner, J. Chem. Soc., Chem. Comm., (1984) 956; M. Brookhart, D. Timmers, J.R. Tucker, G.D. Williams, G.R. Husk, H. Brunner and B. Hammer, J. Am. Chem. Soc., 105 (1983) 6721; J.W. Faller and K.H. Chao, J. Am. Chem. Soc., 105 (1983) 3893; J.W. Faller and K.H. Chao, Organometallics 3 (1984) 927; J.W. Faller and D.L. Linebarrier, J. Am. Chem. Soc., 111 (1989) 1937; J.W. Faller, J.A. John and M.R. Mazzieri, Tetrahedron Lett., 30 (1989) 1769.

2 H. Brunner, C.R. Jablonski and P.G. Jones, Organometallics, 7 (1988) 1283; C.R. Jablonski, T. Burrow and P.G. Jones, J. Organomet. Chem., 370 (1989) 173; C.R. Jablonski and H. Ma, 74th Canadian Chemical Conference and Exhibition, Hamilton, Ontario, Abstracts, IN-390, 1991.

3 E.L. Eliel, The Stereochemistry of Carbon Compounds, McGraw-Hill, New York, 1962, p. 63.

4 H. Brunner, J. Doppelberger, P. Dreischel and T. Moellenberg, J. Organomet. Chem., 139 (1977) 223.

5 R.T. Baker and T.H. Tulip, Organometallics, 5 (1986) 839 and references therein; S.A. Westcott, A.K. Kakkar, G. Stringer, N.J. Taylor and T.B. Marder, J. Organomet. Chem., 394 (1990) 777.

6 R.S. Cahn, C. Ingold and V. Prelog, Angew. Chem., Int. Ed. Engl., 5 (1966) 385; K. Stanley and M.C. Baird, J. Am. Chem. Soc., 97 (1975) 6598; T.E. Sloan, Top. Stereochem., 12 (1981) 1.

7 J.K.M. Sanders and J.D. Mersh, Prog. Nucl. Magn. Res. Spec., 15 (1983) 353.

8 H. Brunner, G. Riepl, R. Benn and A. Rufinska, J. Organomet. Chem., 253 (1983) 93.

9 Kinetic studies of Co epimerization in related chiral CpCo*(PNH*)(X)I complexes show similar results. C.R. Jablonski and N. Brunet, unpublished results.

10 H. Bönnemann and W. Brijoux, in R. Ugo (Ed.), Aspects of Homogeneous Catalysis, Vol. 5, 1984, p. 75.

11 A. Salzer and C. Täschler, J. Organomet. Chem., 294 (1985) 261.